Inorg. Chem. **2008**, *47*, 4199−4208

New Attempt at Directly Generating Superbasicity on Mesoporous Silica SBA-15

Lin Bing Sun,[†] Jia Hui Kou,[‡] Yuan Chun,[†] Jing Yang,[†] Fang Na Gu,[†] Ying Wang,[‡] Jian Hua Zhu,*[,†] and Zhi Gang Zou[‡]

Key Laboratory of Mesoscopic Chemistry of MOE, School of Chemistry and Chemical Engineering, and Ecomaterials and Renewable Energy Research Center (ERERC), Nanjing University, Nanjing 210093, China

Received November 12, 2007

Direct generation of superbasicity on mesoporous silica SBA-15 was realized by tailoring the host–guest interaction, and calcium species were selected as the guest in modifying SBA-15. The results show that calcium species could be homogeneously distributed on the surface of SBA-15. Because of the host–guest interaction, the decomposition of the supported calcium nitrate was apparently easier than the bulk one. Surprisingly, the calcium nitrates modified SBA-15 (CaNS) samples exhibited superbasicity with good preservation of the mesostructure after activation, differing from the potassium nitrate loaded SBA-15 samples that displayed weak basicity with collapsed mesostructure. The present superbasic CaNS materials also possess good water resistance and high surface areas, up to 429 $m^2\ g^{-1}$, which is promising for their potential applications in adsorption and catalysis. Further investigation concerning the roles played by the guest in basicity formation on SBA-15 was conducted. The samples modified by Group 2 metal nitrates showed strong basicity with base strength (H_-) of 22.5–27.0 and good preservation of mesostructure. In contrast, loading Group 1 metal nitrates on SBA-15 produced samples with weak basicity ($H_- = 9.3$–15.0) and collapsed mesostructure after activation. Such differences can be related to the interaction between the resulting metal oxide and the silica support, as well as the mobility of the cations in the metal oxide.

Introduction

Solid strong bases, especially those with ordered pore structure, are highly promising for a range of potential applications in the chemical industry because they can catalyze diverse reactions under mild conditions and reduce the production of pollutants.[1–3] Among various porous materials, zeolites are able to recognize, discriminate, and organize molecules with excellent precision.[4] Consequently, much attention has been paid to the preparation of shape-selective basic materials derived from zeolites.[5–9] However, the small pore openings of zeolites prevents bulky molecules from reaching the active sites, which limits their applications. Since the discovery of ordered mesoporous silica M41S, a variety of ordered mesoporous materials have been synthesized using the surfactant templating method.[10,11] These mesoporous materials possess higher surface areas and pore volumes than zeolites, which is of great interest for separation, sensing, and catalysis.[12–16] The complementary use of

* To whom correspondence should be addressed. E-mail: jhzhu@nju.edu.cn. Phone: +86-25-83595848. Fax: +86-25-83317761.
[†] School of Chemistry and Chemical Engineering.
[‡] Ecomaterials and Renewable Energy Research Center (ERERC).

(1) Ono, Y. *J. Catal.* **2003**, *216*, 406.
(2) Weitkamp, J.; Hunger, M.; Rymsa, U. *Microporous Mesoporous Mater.* **2001**, *48*, 255.
(3) Hattori, H. *Chem. Rev.* **1995**, *95*, 537.
(4) Davis, M. E. *Acc. Chem. Res.* **1993**, *26*, 111.
(5) Hathaway, P. E.; Davis, M. E. *J. Catal.* **1998**, *119*, 497.
(6) Kim, J. C.; Li, H. X.; Chen, C. Y.; Davis, M. E. *Microporous Mater.* **1994**, *2*, 413.
(7) Baba, T.; Kim, G. J.; Ono, Y. *J. Chem. Soc., Faraday Trans.* **1993**, *88*, 891.
(8) Baba, T.; Hikita, S.; Koide, R.; Ono, Y. *J. Chem. Soc., Faraday Trans.* **1993**, *89*, 3177.
(9) Zhu, J. H.; Chun, Y.; Wang, Y.; Xu, Q. H. *Mater. Lett.* **1997**, *33*, 207.
(10) Kresge, C. T.; Leonowicz, M. E.; Roth, W. J.; Vartuli, J. C.; Beck, J. S. *Nature* **1992**, *359*, 710.
(11) Beck, J. S.; Vartuli, J. C.; Roth, W. J.; Leonowicz, M. E.; Kresge, C. T.; Schmitt, K. D.; Chu, C. T. W.; Olson, D. H.; Sheppard, E. W.; McCullen, S. B.; Higgins, J. B.; Schlenker, J. L. *J. Am. Chem. Soc.* **1992**, *114*, 10834.
(12) De Vos, D. E.; Dams, M.; Sels, B. F.; Jacobs, P. A. *Chem. Rev.* **2002**, *102*, 3615.
(13) Davis, M. E. *Nature* **2002**, *417*, 813.
(14) Stein, A. *Adv. Mater.* **2003**, *15*, 763.
(15) Scott, B. J.; Wirnsberger, G.; Stucky, G. D. *Chem. Mater.* **2001**, *13*, 3140.

10.1021/ic702223b CCC: $40.75
Published on Web 04/17/2008

mesoporous materials as carriers for the preparation of solid bases is also expected. In contrast to other candidates with mesostructure, mesoporous silicas are easier to synthesize and have better stability. So far an incredible degree of control can be achieved on silica with various pore symmetries, such as hexagonal, cubic, lamellar, and wormhole.[17–20] Therefore, mesoporous silicas should be the suitable starting materials for the preparation of strong basic materials. Up to now, many attempts have been made to generate strong basicity on mesoporous silicas. For instance, mesoporous solid strong bases can be prepared by impregnation of MCM-41 with cesium acetate solution and subsequent calcination.[21] However, the obtained bases showed poor thermal and chemical stability because the cesium oxide can react with silica and damage the framework of the host.[22] Through treating the ordered mesoporous silicas such as MCM-41 and SBA-15 in the presence of ammonia or nitrogen, the oxygen in their frameworks was partially displaced by nitrogen or NH_x species to generate oxynitride frameworks, which afforded new types of solid bases with ordered mesostructure.[23,24] Nevertheless, the treatment temperature was usually higher than 900 °C, and the strength of the basic sites still needed further improvement. Anchoring organic bases at the silanol groups provided an interesting approach to create basic sites on mesoporous silicas, but the preparation of these organic–inorganic hybrid materials was rather complicated and expensive.[25–27] Also, they can only be applied at temperatures lower than 170 °C because of the degradation of the organic molecules at higher temperatures.[2] Hence, it is still a challenge to generate strong basicity on mesoporous silicas so far.

In previous investigations, neutral salt KNO_3 has been used as a base precursor to disperse on porous supports such as Al_2O_3, ZrO_2, and zeolite KL, which provides a facile and low-cost method to prepare solid superbases.[9,28–30] Because the superbasic sites are only generated by the in situ activation prior to reaction, the contamination with atmospheric CO_2 can be avoided. Therefore, these solid bases are easy to store and efficient in catalytic processes.[29,30] Aiming at generating superbasicity on mesoporous silicas, SBA-15 was employed as a host into which to disperse the guest KNO_3. Unfortunately, the obtained sample exhibited weak basicity and the mesostructure of SBA-15 was destroyed completely during the activation to decompose the supported KNO_3.[31] To overcome this disadvantage, SBA-15 was precoated with a layer of MgO, before KNO_3 modification, to prevent the reaction of the resulting basic potassium species with silica.[31] As a result, superbasic sites were successfully generated with good preservation of mesostructure. Nonetheless, the procedure for tailoring the host is relatively complicated, and the surface area of SBA-15 decreases after precoating with MgO. In contrast to the host, however, the importance of the guest is often neglected. Up to now, few attempts have been made to generate strong basic sites on mesoporous silicas by adjusting the guest species, for example, by using calcium species instead of potassium species. In comparison with Group 1 metal oxides, less attention has been paid to the application of Group 2 metal oxides as basic species to modify mesoporous silicas. Metal oxides from Groups 1 and 2 are recognized basic species, and their different physicochemical properties may lead to quite different characteristics of the resulting bases. Thus, it is valuable to clarify the possibility of producing strong basic sites on mesoporous silicas by the modification of guest species from Group 2. Also, it is desirable to investigate the effect of different precursors from Groups 1 and 2 on the basicity and mesostructure of these modified mesoporous silicas, which is meaningful to the preparation of new basic materials.

In the present study, we tried to introduce a new guest, calcium species, to modify mesoporous silica SBA-15. The resulting composites exhibited superbasicity with good preservation of mesostructure after activation, which was quite different from potassium species modified SBA-15 samples. The structure of the new mesoporous solid superbases was characterized by X-ray diffraction (XRD), N_2 adsorption, and transmission electron microscopy (TEM). The decomposition behavior of calcium nitrate on SBA-15 and the resulting basicity were studied in detail. Aiming at clarifying the roles of the guest played in basicity formation on mesoporous silica, a series of metal nitrates from Groups 1 and 2 were also employed to modify SBA-15, and various basic and textual characteristics of these metal nitrates modified SBA-15 were examined to assess the factors influencing the generation of strong basicity and the preservation of mesostructure. A correlation of guest properties with basicity and structure was also proposed.

Experimental Section

The mesoporous silica SBA-15 was prepared according to the literature.[32] In a typical synthesis, 2 g of triblock copolymer P123 ($EO_{20}PO_{70}EO_{20}$) was dissolved in 60 g of 2 M HCl aqueous solution

(16) Wang, Y. M.; Wu, Z. Y.; Shi, L. Y.; Zhu, J. H. *Adv. Mater.* **2005**, *17*, 323.
(17) Asefa, T.; MacLachan, M. J.; Coombs, N.; Ozin, G. A. *Nature* **1999**, *402*, 867.
(18) Liu, X. Y.; Tian, B. Z.; Yu, C. Z.; Gao, F.; Xie, S. H.; Tu, B.; Che, R. C.; Peng, L. M.; Zhao, D. Y. *Angew. Chem., Int. Ed.* **2002**, *41*, 3876.
(19) Kim, S. S.; Zhang, W. Z.; Pinnavaia, T. J. *Science* **1998**, *282*, 1302.
(20) Mercier, L.; Pinnavaia, T. J. *Adv. Mater.* **1997**, *9*, 500.
(21) Kloetstra, K. R.; van Bekkum, H. *Stud. Surf. Sci. Catal.* **1997**, *105*, 431.
(22) Kloetstra, K. R.; van Laren, M.; van Bekkum, H. *J. Chem. Soc., Faraday Trans.* **1997**, *93*, 1211.
(23) Xia, Y.; Mokaya, R. *Angew. Chem., Int. Ed.* **2003**, *42*, 2639.
(24) Wang, J.; Liu, Q. *Microporous Mesoporous Mater.* **2005**, *83*, 225.
(25) Macquarrie, D. J.; Jackson, D. B.; Tailland, S.; Utting, K. A. *J. Mater. Chem.* **2001**, *11*, 1843.
(26) Wang, X.; Lin, K. S. K.; Chan, J. C. C.; Cheng, S. *Chem. Commun.* **2004**, 2762.
(27) Wang, X.; Lin, K. S. K.; Chan, J. C. C.; Cheng, S. *J. Phys. Chem. B* **2005**, *109*, 1763.
(28) Yamaguchi, T.; Zhu, J. H.; Wang, Y.; Komatsu, M.; Ookawa, M. *Chem. Lett.* **1997**, *10*, 989.
(29) Zhu, J. H.; Wang, Y.; Chun, Y.; Wang, X. S. *J. Chem. Soc., Faraday Trans.* **1998**, *94*, 1163.
(30) Wang, Y.; Huang, W. Y.; Chun, Y.; Xia, J. R.; Zhu, J. H. *Chem. Mater.* **2001**, *13*, 670.
(31) Wu, Z. Y.; Jiang, Q.; Wang, Y. M.; Wang, H. J.; Sun, L. B.; Shi, L. Y.; Xu, J. H.; Wang, Y.; Chun, Y.; Zhu, J. H. *Chem. Mater.* **2006**, *18*, 4600.
(32) Zhao, D. Y.; Feng, J. L.; Huo, Q. S.; Melosh, N.; Fredrickson, G. H.; Chmelka, B. F.; Stucky, G. D. *Science* **1998**, *279*, 548.

with stirring at 40 °C. Then, 4.25 g of tetraethylorthosilicate (TEOS) was added to the homogeneous solution and stirred at this temperature for 24 h. Finally, the temperature was heated to 130 °C and held at this temperature for 24 h under static conditions. The as-prepared sample was recovered by filtration, washed with water, and air-dried at room temperature. The removal of the template was carried out at 550 °C in air for 5 h.

The base precursor $Ca(NO_3)_2$ was loaded on SBA-15 by impregnation with aqueous solution of $Ca(NO_3)_2$ for 24 h. After evaporation of the solvent, the resulting solid was dried at 100 °C overnight to give the sample denoted as *n*CaNS, where *n* represents the weight percentage of $Ca(NO_3)_2$. In similar a process, $NaNO_3$, KNO_3, $CsNO_3$, $Mg(NO_3)_2$, $Sr(NO_3)_2$, and $Ba(NO_3)_2$ were loaded on SBA-15 with the same surface cation density (2.1 nm^{-2}) as that of 30CaNS. The obtained composites were denoted as NaNS, KNS, CsNS, MgNS, SrNS, and BaNS, respectively. After the composites were activated in N_2 at 550 °C for 2 h, their structures were detected by XRD, TEM, and N_2 adsorption methods. XRD patterns of the samples were recorded with a Rigaku D/max-rA system using Cu Kα radiation in the 2θ ranges from 0.6° to 8° and 5° to 80° at 40 kV and 40 mA. TEM and energy dispersive X-ray (EDX) analysis were performed on a FEI Tecnai G^2 20 S-TWIN electron microscope operated at 200 kV. The N_2 adsorption–desorption isotherms were measured using a Micromeritics ASAP 2020 system at −196 °C. The samples were outgassed at 300 °C for 4 h prior to analysis. The Brunauer–Emmett–Teller (BET) surface area was calculated using adsorption data in a relative pressure ranging from 0.04 to 0.20. The total pore volume was determined from the amount adsorbed at a relative pressure of about 0.99. The pore diameter was calculated from the adsorption branch by using the Kruk−Jaroniec−Sayari (KJS) method.[33]

Fourier transform infrared (FTIR) measurements were performed on a Bruker 22 FTIR spectrometer by means of the KBr pellet technique. Each wafer with a diameter of 13 mm consisted of about 0.4 mg of sample and 19.6 mg of KBr. The spectra were collected with a 2 cm^{-1} resolution. The element contents of the composites were measured by a ARL-9800 X-ray fluorescence (XRF) spectrometer. Thermogravimetry-mass spectrometry (TG-MS) analysis was conducted on a thermobalance (STA-499C, NETZSCH) coupled to a mass analyzer (QUADSTAR-422, PFEIFFER). The sample (ca. 10 mg) was heated from 25 to 900 at 8 °C·min^{-1} in a continuous flow of Ar (30 mL·min^{-1}). The ionization of the decomposition products was performed with an ion source of electron impact at 70 eV. Temperature programmed decomposition (TPDE) of $Ca(NO_3)_2$ on SBA-15 was carried out in a flow reactor. The NO_2 derived from $Ca(NO_3)_2$ decomposition was detected by a colorimetric method.[30] To determine the liberated NO, the gaseous products were passed through a CrO_3 tube to convert NO to NO_2 before measurement. The total amount of NO_x was used to represent the nitrate decomposed.

In a temperature programmed desorption (TPD) of CO_2 experiment, the adsorption of CO_2 was conducted at 25 °C after the sample was activated at 550 °C for 2 h. CO_2-TPD was performed by using a TG-MS apparatus, and the analysis conditions were similar to those described above. The *m*/*z* value of 44 was used to represent the CO_2 desorbed. The base strength of the sample was detected by using a series of Hammett indicators, for which the samples (ca. 100 mg) were activated in a N_2 flow with 30 mL·min^{-1} at 550 °C for 2 h before the test. The indicators employed were phenolphthalein (H_- = 9.3), 2,4-dinitroaniline (H_- = 15.0), 4-nitroaniline (H_- = 18.4), benzidine (H_- = 22.5), 4-chloroaniline (H_- = 26.5), and aniline (H_- = 27.0). To measure the basicity, 100 mg of sample after activation was shaken in 10 mL of aqueous HCl (0.20 M) for 24 h, and the slurry was separated by a centrifuge. The remained acid in the liquid phase was titrated with standard base (0.05 M aqueous NaOH), and phenolphthalein was employed as an indicator. The amount of HCl consumed was utilized to denote the basicity. To check the dissolution of calcium species in the detection of basicity, the solution before titration was analyzed by a J-A1100 inductively coupled plasma-optical emission spectrometry (ICP-OES). After the sample was activated in N_2 at 550 °C (600 °C for the sample of $20KNO_3/Al_2O_3$) for 2 h, the water-resistance was measured as reported previously.[34]

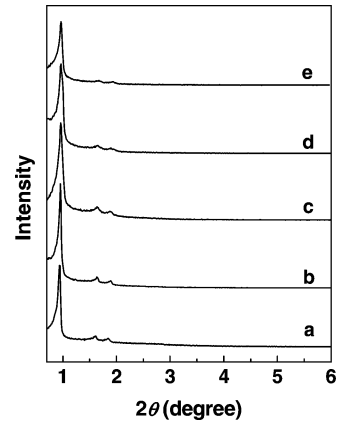

Figure 1. Low-angle XRD patterns of (a) SBA-15, (b) 10CaNS, (c) 20CaNS, (d) 30CaNS, and (e) 40CaNS. The CaNS samples were activated in N_2 at 550 °C prior to measurement.

Results

Characterization of Mesoporous Solid Strong Bases Using Calcium Species As Guest. Figure 1 shows the low-angle XRD patterns of the parent SBA-15 and CaNS samples. All samples have a very intense diffraction line at 2θ of 0.9° accompanied by two weak lines at 2θ of 1.6° and 1.9° indexed as (100), (110), and (200) reflections, respectively, corresponding to a two-dimensional hexagonal pore regularity of a *P6mm* space group.[32] This indicates the preservation of the ordered mesopores of SBA-15 silica, even if $Ca(NO_3)_2$ was introduced and converted to a strong basic species CaO after activation. In general, the intensity of the (100) reflection should decline with the introduction of metal oxides because of the decreasing scatter contrast between pore walls and pore space. Surprisingly, the intensity of the (100) reflection of the samples containing 10–30 wt % $Ca(NO_3)_2$ was obviously stronger than that of the parent SBA-15. Because the samples were obtained through impregnation rather than direct synthesis, factors such as salt effect derived from synthesis process should be excluded. As a result, the reflection enhancement can be tentatively ascribed to the formation of a smooth CaO layer on the internal walls of SBA-15. Such a smooth layer contributes to the spatial order giving rise to the diffraction pattern itself and results in less-blocked mesopores, similar to that found in magnesia or yttria modified SBA-15.[35,36]

(33) Jaroniec, M.; Solovyov, L. A. *Langmuir* **2006**, *22*, 6757.

(34) Wei, Y. L.; Wang, Y. M.; Zhu, J. H.; Wu, Z. Y. *Adv. Mater.* **2003**, *15*, 1943.

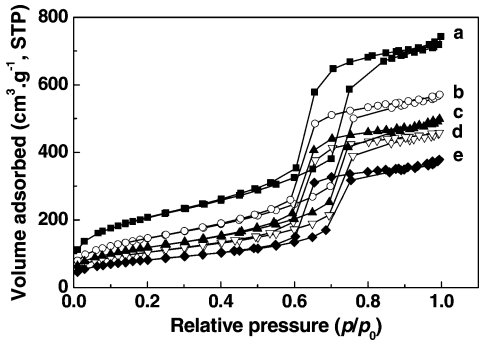

Figure 2. N_2 adsorption–desorption isotherms of (a) SBA-15, (b) 10CaNS, (c) 20CaNS, (d) 30CaNS, and (e) 40CaNS. The CaNS samples were activated in N_2 at 550 °C prior to measurement.

Figure 2 depicts the N_2 adsorption–desorption isotherms of SBA-15 and CaNS samples. The isotherms of the CaNS samples were of type IV with an H1 hysteresis loop, quite similar to that of the parent SBA-15. However, the onset of the inflections slightly shifted toward lower p/p_0 values, and the amount of adsorbed N_2 decreased, which originated from the loading of the guest in SBA-15. As shown in Table 1, both the surface area and the pore volume decreased gradually with the increasing amount of calcium in the samples. However, the pore diameter was reduced less than the pore volume with the increase of the calcium content. As described above, the supported CaO could form a smooth layer on the internal walls of SBA-15, which led to less-blocked mesopores. Hence, the decrease of the pore diameter was relatively small, similar to the phenomenon observed in MgO-modified SBA-15 samples.[31,34] Nonetheless, the adsorption amount declined with the increase of calcium content (Figure 2), which implied the obstruction of some primary pores by CaO despite the lesser reduction of the main pore diameter. It is worth noticing that some superbasic sites ($H_- = 27.0$) emerged on the samples with $Ca(NO_3)_2$ loading over 20 wt % (Table 1). This is the first time that superbasic sites were generated directly on the mesoporous silica. Moreover, the 20CaNS sample had a large surface area of 429 $m^2 \cdot g^{-1}$ and pore volume of 0.745 $cm^3 \cdot g^{-1}$. In the previous report, we have prepared the multicoated solid superbase, that is, KNO_3 loaded on MgO-coated SBA-15 (KMS).[31] The KMS sample possessed a surface area of 223 $m^2 \cdot g^{-1}$ and a pore volume of 0.39 $cm^3 \cdot g^{-1}$, which was much smaller than that of the CaNS samples. Therefore, the present superbasic CaNS materials with mesostructure and high surface area offer a new candidate for selective adsorption and catalysis.

TEM provides another important technique to characterize the long-range channel ordering. As illustrated in Figure 3A, the mesostructure was preserved in the CaNS sample, being consistent with the results of XRD and N_2 adsorption. EDX analysis was performed to estimate the local element composition of the 30CaNS sample. As shown in Figure 3B, the calcium and silicon signals can be clearly identified. Although several random areas were selected for EDX analysis, the resultant Ca/Si atomic ratios were similar, indicating a homogeneous distribution of calcium species on the surface of SBA-15.

Figure 4 presents the wide-angle XRD patterns of SBA-15 and CaNS samples recorded at different conditions. For parent SBA-15, only a broad peak with a 2θ value of 22° assigned to amorphous silica was detected. No new diffraction lines appeared on the sample of 10CaNS and 20CaNS, suggesting a good dispersion of the calcium salt. However, a wide and inconspicuous peak with a 2θ value of 41° originating from $Ca(NO_3)_2$ (JCPDS card 07–0204) emerged on the composite when the loading amount of $Ca(NO_3)_2$ rose to 30 wt %. Further increasing the $Ca(NO_3)_2$ loading to 40 wt % on SBA-15 enhanced the peak intensity. These results imply that the monolayer dispersion threshold of $Ca(NO_3)_2$ on SBA-15 is below 30 wt %. Assuming that each $Ca(NO_3)_2$ molecule exists in the cubic form and its coverage is around 0.56 nm^2,[37] for SBA-15 with a surface area of 747 $m^2 \cdot g^{-1}$, about 26 wt % of $Ca(NO_3)_2$ can be dispersed as a monolayer theoretically, which is in good agreement with the practical value. In addition, the wide and weak diffraction peak indicates that the $Ca(NO_3)_2$ phase consists of small particles.

Decomposition of Calcium Nitrate on SBA-15 and the Resulting Basicity. As shown in Table 1, the atomic ratio of Ca/Si in different samples was measured by XRF. The detected values were in accord with the calculated ones, indicating that the calcium added is recovered well during sample synthesis. Moreover, the Ca/Si ratio kept constant even though the CaNS sample was activated at 550 °C. As is evident in Figure 4 (curve f), the XRD diffraction peak of $Ca(NO_3)_2$ on 40CaNS disappeared after activation. Since the evaporation of the supported calcium salt is excluded from the results of XRF, the disappearance of the diffraction peak can be ascribed to either dispersion or decomposition of $Ca(NO_3)_2$ in the process of thermal treatment. Figure 5 gives the IR spectra of the samples after different pretreatment. For the samples containing $Ca(NO_3)_2$, a strong band at 1384 cm^{-1} was observed, which could be ascribed to the asymmetric stretching vibration N—O of the nitrate.[38] When the loading amount of $Ca(NO_3)_2$ varied from 10 to 30 wt %, the band intensity of the nitrate increased apparently. After the activation at 550 °C, the band of nitrate disappeared in the spectra of the CaNS samples. Because IR is able to detect the existence of a compound whether it is in the form of crystal or not, the vanishing of the nitrate band should be related to the decomposition rather than to the dispersion of the calcium salt, which is also responsible for the aforementioned disappearance of the $Ca(NO_3)_2$ diffraction peak in the XRD pattern. According to the results of XRD and IR, it is clear that $Ca(NO_3)_2$ supported on SBA-15 can be decomposed completely using thermal activation at 550 °C in N_2 for 2 h. This is important for the preparation of solid bases

(35) Sauer, J.; Marlow, F.; Schuth, F. *Phys. Chem. Chem. Phys.* **2001**, *3*, 5579.
(36) Wang, Y. M.; Wu, Z. Y.; Wei, Y. L.; Zhu, J. H. *Microporous Mesoporous Mater.* **2005**, *84*, 127.
(37) Xu, Y.; Jiang, Q.; Cao, Y.; Wei, Y. L.; Yun, Z. Y.; Xu, J. H.; Wang, Y.; Zhou, C. F.; Shi, L. Y.; Zhu, J. H. *Adv. Funct. Mater.* **2004**, *14*, 1113.
(38) Sun, L. B.; Chun, Y.; Gu, F. N.; Yue, M. B.; Yu, Q.; Wang, Y.; Zhu, J. H. *Mater. Lett.* **2007**, *61*, 2130.

Table 1. Physicochemical Characteristics of SBA-15 and CaNS Samples

	atomic ratio of Ca/Si						basicity (mmol(OH^{-1})·g^{-1})[d]		
sample	calculated	detected[a]	S_{BET}[c] ($m^2 \cdot g^{-1}$)	V_p[c] ($cm^3 \cdot g^{-1}$)	D_p[c] (nm)	base strength (H_-)	A	B	C
SBA-15	0	0	747	1.097	7.67	<9.3	0	0	0
10CaNS	0.04	0.04	528	0.861	7.63	18.4	1.22	1.07	1.02
20CaNS	0.09	0.11	429	0.745	7.58	27.0	2.44	2.15	2.01
30CaNS	0.16	0.17 (0.16[b])	375	0.693	7.57	27.0	3.66	3.22	3.07
40CaNS	0.24	0.26	296	0.564	7.42	27.0	4.88	4.29	4.27

[a] Data from XRF. [b] The sample was activated in N_2 at 550 °C before measurement. [c] S_{BET}, BET surface area; V_p, total pore volume; D_p, pore diameter calculated from the adsorption branch. [d] A, theoretical value (twice the amount of calcium in the sample); B, corrected value for hydrated sample; C, detected value.

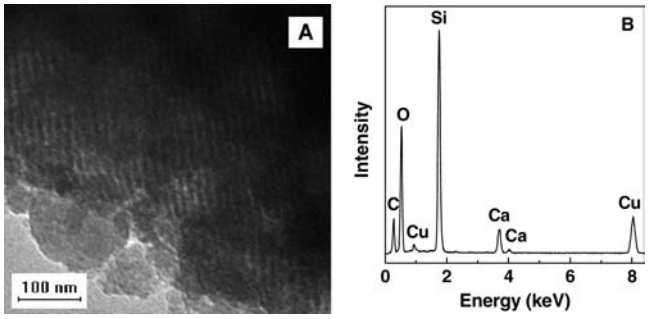

Figure 3. (A) TEM image and (B) EDX spectrum of 30CaNS. The sample was activated in N_2 at 550 °C before measurement.

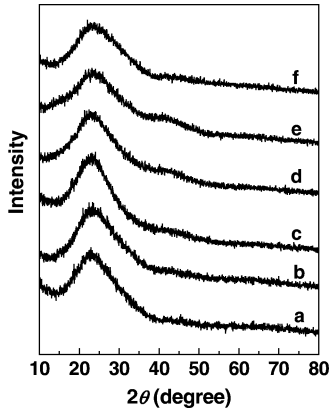

Figure 4. Wide-angle XRD patterns of (a) SBA-15, (b) 10CaNS, (c) 20CaNS, (d) 30CaNS, and (e) 40CaNS before activation, and (f) 40CaNS after activation in N_2 at 550 °C.

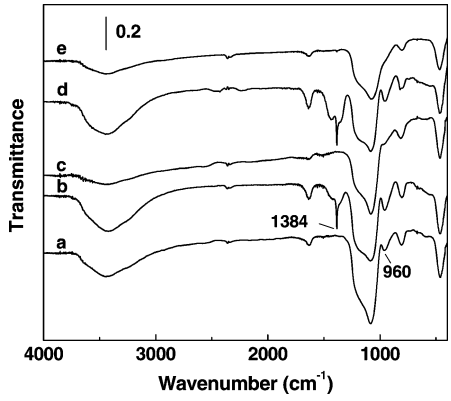

Figure 5. IR spectra of (a) SBA-15, 10CaNS (b) before and (c) after activation in N_2 at 550 °C as well as the 30CaNS sample (d) before and (e) after activation in N_2 at 550 °C.

because $Ca(NO_3)_2$ is neutral and the basic sites of the samples only generate after the decomposition of calcium salt.

The interaction of the supported oxide species with the silica surface will consume silanol groups (Si−OH); therefore, the alteration of the silanol groups was monitored by IR analysis. In theory, the stretching and bending vibrations of Si−OH give rise to the bands at about 3750 and 960 cm^{-1}, respectively. Actually, the band at 3750 cm^{-1} is often invisible because of the influence of the adsorbed water that presents a broadband at around 3430 cm^{-1}.[36,39,40] Hence, the bending vibration band at 960 cm^{-1} was employed to reflect the alteration of the silanol groups. The band at 960 cm^{-1} in the most ordered mesoporous materials indicates the presence of perturbing or defect groups, which was observed on parent SBA-15 and $Ca(NO_3)_2$ modified SBA-15 samples as delineated in Figure 5. For the sample of 10CaNS, the 960 cm^{-1} band decreased apparently after activation. Increasing the loading amount of $Ca(NO_3)_2$ to 30 wt %, the band degraded to the shoulder of the 1080 cm^{-1} band after activation. These results indicate that the activation at high temperature suppressed the surface silanol groups of the samples. The consumption of silanol groups by the interaction of the supported oxides and SBA-15 has been widely investigated.[31,36,40,41] According to the interaction between oxides and SBA-15, the oxides can be divided into two kinds. If the supported oxides, for example, NiO and Cr_2O_3, show a weak interaction with the support, then the silanol groups can be well preserved. The oxides of this kind are easy to aggregate and exhibit crystalline phases in XRD patterns.[36] The other kind of oxides, for example, MgO and ZnO, prefer to interact with the silanol groups, which results in good dispersion of oxides on the surface of SBA-15 and the absence of crystalline oxides in XRD patterns.[36,40] As a result, CaO can be tentatively assigned to the oxide of the latter kind, and the interaction between CaO and SBA-15 will lead to the consumption of silanol groups. This point is confirmed by the XRD results because the supported CaO can be well dispersed and no crystalline phases were observed (curve f, Figure 4).

The decomposition of $Ca(NO_3)_2$ on SBA-15 was studied by means of a TPDE method. As seen in Figure 6 and Table 2, bulk $Ca(NO_3)_2$ started to decompose at 500 °C and presented a unique and sharp peak centered at 600 °C. After being supported on SBA-15, $Ca(NO_3)_2$ exhibited a different decomposition behavior. The supported $Ca(NO_3)_2$ began to decompose at a temperature as low as 200 °C while the peak maximum varied with the calcium content. Only one peak

(39) Tian, B.; Liu, X.; Yu, C.; Gao, F.; Luo, Q.; Xie, S.; Tu, B.; Zhao, D. *Chem. Commun.* **2002**, 1186.
(40) Jiang, Q.; Wu, Z. Y.; Wang, Y. M.; Cao, Y.; Zhou, C. F.; Zhu, J. H. *J. Mater. Chem.* **2006**, *16*, 1536.
(41) Wang, Y. M.; Wu, Z. Y.; Zhu, J. H. *J. Solid State Chem.* **2004**, *177*, 3815.

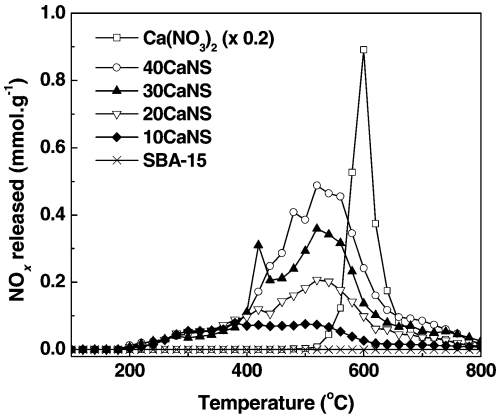

Figure 6. TPDE patterns of $Ca(NO_3)_2$ unsupported and supported on SBA-15.

Table 2. TPDE Results of $Ca(NO_3)_2$ Unsupported and Supported on SBA-15

	peak max (°C)		NO_x released (mmol·g^{-1}) at different temperature (°C)		
sample	T_1	T_2	$200 \le T <$ 400 (I)	$400 \le T <$ 600 (II)	$600 \le T <$ 800 (III)
10CaNS	380		0.407 (33.3%)[a]	0.664 (54.1%)	0.154 (12.6%)
20CaNS	420	520	0.432 (18.0%)	1.538 (63.7%)	0.443 (18.3%)
30CaNS	420	520	0.358 (9.6%)	2.625 (70.9%)	0.723 (19.5%)
40CaNS	480	520	0.424 (8.8%)	3.356 (70.0%)	1.018 (21.2%)
$Ca(NO_3)_2$		600	0 (0%)	3.531 (29.1%)	8.586 (70.9%)

[a] The numeral in parenthesis denotes the percentage of $Ca(NO_3)_2$ decomposed.

at 380 °C could be identified in the decomposition curve of 10CaNS. With the increase of the calcium content, the peak maximum had a tendency to enhance, and another peak at the higher temperature of 520 °C became visible. To understand the decomposition behavior of $Ca(NO_3)_2$ in detail, the decomposition processes were divided into three stages (Table 2), that is, 200–400 °C (stage I), 400–600 °C (stage II), and 600–800 °C (stage III). In the case of bulk $Ca(NO_3)_2$, more than 70% of the $Ca(NO_3)_2$ is decomposed at stage III along with about 30% that is decomposed at stage II. When $Ca(NO_3)_2$ with 10 wt % was supported on SBA-15, the major amount was decomposed at stages I (33.3%) and II (54.1%) with the minor amount at stage III (12.6%). Increasing the calcium loading made the percentage of $Ca(NO_3)_2$ decomposed at stage I decrease whereas that at stages II and III increased. These results are indicative of the interaction between SBA-15 and $Ca(NO_3)_2$, and such interaction can promote the decomposition of supported nitrate so that the decomposition temperature of $Ca(NO_3)_2$ is lowered on SBA-15. Furthermore, with the increase of $Ca(NO_3)_2$ loading, the decomposition seemed to be difficult, which should be associated with the dispersion state of $Ca(NO_3)_2$ on SBA-15. In other words, $Ca(NO_3)_2$ with a lesser loading amount can be dispersed better on SBA-15, which is beneficial to the subsequent decomposition.

To gain a deeper insight into the decomposition of $Ca(NO_3)_2$ on SBA-15, the TG-MS technique was employed. Figure 7 displays the TG curve and the mass analysis of the 30CaNS sample. The first weight loss centered at about 100 °C was assigned to water referring to the MS signal of $m/z = 18$. In the temperature ranging from 200 to 800 °C, there

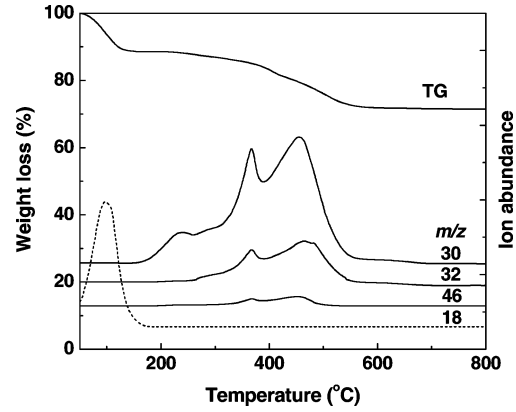

Figure 7. TG curve and mass analysis of the 30CaNS sample.

were several gradual but constant weight losses, which can be attributed to the decomposition of supported $Ca(NO_3)_2$, as confirmed by the following MS analysis. According to the TG curve, the weight loss derived from the $Ca(NO_3)_2$ decomposition was calculated to be 17.2%, in agreement with the theoretical value (19.8%). Among the mass signals derived from $Ca(NO_3)_2$ decomposition, the m/z values of 32 and 46 are characteristic of O_2 and NO_2, respectively. However, it is inappropriate to simply attribute the m/z value of 30 to the primary product NO because the decomposition of NO_2 to NO can occur in the detection procedure of MS.[42,43] In other words, NO_2 is also a possible origin for the mass signal of $m/z = 30$. Therefore, a colorimetric method, in which the conversion of NO_2 to NO that usually occurrs in MS can be avoided, was applied to examine whether NO or NO_2 was produced from the decomposition of the supported $Ca(NO_3)_2$. The patterns from the colorimetric method (data not shown) displayed similar change trends of nitrogen oxides liberation as those from MS; however, in which NO_2 was mainly detected along with negligible amount of NO, implying that the signal of $m/z = 30$ in TG-MS analysis predominantly came from NO_2 cracking. Therefore, the decomposition of $Ca(NO_3)_2$ on SBA-15 mainly produced NO_2 and O_2, which can be described by the following equation: $Ca(NO_3)_2 = CaO + 2NO_2 + 0.5O_2$.

The base strength and the basicity of the samples are presented in Table 1. For SBA-15, the base strength (H_-) of less than 9.3 was detected and no basicity was titrated at all. After loading 10 wt % of $Ca(NO_3)_2$, the base strength of the composite was improved obviously, and some strong basic sites with strength (H_-) of 18.4 emerged after activation. It was noticeable that the high base strength of $H_- = 27.0$ was measured when further increasing the amount of $Ca(NO_3)_2$ to 20 wt %. Moreover, varying the amount of $Ca(NO_3)_2$ from 20 to 40 wt % did not influence such a high base strength ($H_- = 27.0$) of the CaNS samples. According to the definition of Tanabe and Noyori, a solid material that possesses the basic sites with strength (H_-) higher than 26.5

(42) Yamaguchi, T.; Wang, Y.; Komatsu, M.; Ookawa, M. *Catal. Surv. Jpn.* **2002**, *5*, 81.
(43) Yamaguchi, T.; Ookawa, M. *Catal. Today* **2006**, *116*, 191.

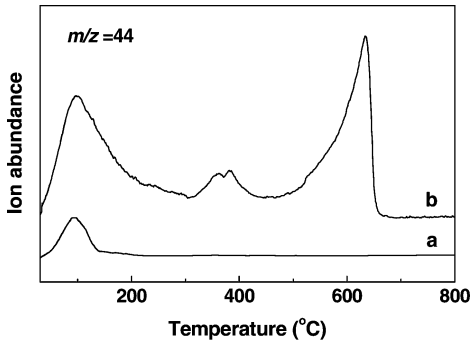

Figure 8. CO_2-TPD profiles of (a) SBA-15 and (b) 30CaNS sample detected by TG-MS.

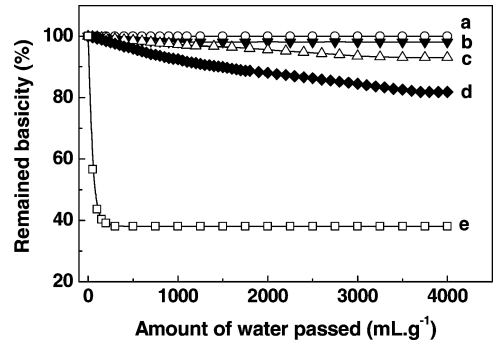

Figure 9. Water-resistance of (a) 10CaNS, (b) 20CaNS, (c) 30CaNS, (d) 40CaNS, and (e) $20KNO_3/Al_2O_3$ samples.

can be regarded as a solid superbase.[44] This is the first evidence of the generation of superbasicity on calcium modified SBA-15 samples. The results of CO_2-TPD further confirm the formation of unusually strong basic sites as shown in Figure 8. The parent SBA-15 possessed a weak ability to adsorb CO_2, and thus, only a little desorption occurred around 90 °C in CO_2-TPD profile. Calcium modification enhanced the basicity of the sample so that the amount of CO_2 desorption at the low temperature increased; additionally, new CO_2 desorption at about 370 and 630 °C appeared. Moreover, the peak of CO_2 desorption at the high temperature of 630 °C was abundant, which provided another evidence on the generation of strong basicity, in good agreement with the results of the base strength. This discovery is of great importance because the direct generation of superbasicity on mesoporous silicas is very difficult.[31] We adopted a facile approach by adjusting the guest species and succeeded in the preparation of the solid superbasic CaNS materials with good preservation of mesostructure.

As shown in Table 1, the basicity of the CaNS samples was enhanced progressively with the increase of the calcium content. To examine if the calcium species went into the solution during the basicity measurement, the solution used for titration was analyzed by ICP. The calcium content in the solution was detected to be 1.58 mmol·g^{-1} for 30CaNS. Taking into consideration that one molecule of calcium reacted with two molecules of HCl, it followed that 3.16 mmol·g^{-1} HCl would be consumed, which is in agreement with the number of basic sites measured (3.07 mmol(OH^{-1})·g^{-1}, Table 1). Therefore, the calcium species dissolved in the HCl solution were responsible for the basicity determined by titration. To establish the relation between the basicity and the amount of calcium, the theoretical calcium amount was calculated according to the $Ca(NO_3)_2$ content of the samples. Here, 30CaNS is taken as an example, and the theoretical calcium amount is 1.83 mmol·g^{-1}. Accordingly, 3.66 mmol·g^{-1} of HCl will be consumed (twice the amount of calcium) and the same amount of basic sites will be measured in theory. Actually, the detected basicity should be smaller because of the existence of moisture in the sample. According to the result of TG-MS (Figure 7), the sample of 30CaNS contained about 12 wt % of water. In other words, the corrected basicity of the hydrated sample should be 88 wt % of the theoretical value, that is, 3.22 mmol(OH^{-1})·g^{-1}, which is close to the experimental value (3.07 mmol(OH^{-1})·g^{-1}, Table 1). Similarly, the corrected basicity of other samples was also in accord with the detected values (Table 1). Hence, the calcium species in the samples act as the basic species, and the detected basicity is consistent with the amount of calcium.

Figure 9 displays the water resistance of some samples. In general, all of the calcium-containing solid bases exhibited excellent water stability, though the remained basicity decreased with the increase of calcium content. About 82% of the basicity survived after 4000 mL·g^{-1} water passed, even for the sample of 40CaNS that exhibited the worst water stability among the CaNS composites. One may argue that the supported CaO could be transformed to $Ca(OH)_2$ during the measurement of the water resistance, which may affect the quantitative analysis of the basicity. Actually, the basicity of the samples was expressed with the amount of OH^-, that is, twice the amount of calcium. Therefore, the basicity should remain constant if no loss of calcium species took place during water washing, although CaO was transformed to $Ca(OH)_2$ upon addition of water. The interaction of the calcium species with the support plays an important role in the water stability of the samples. When the amount of calcium was higher than the monolayer dispersion threshold, the calcium species on the outer layer of the samples could be leached out because of the solubility of $Ca(OH)_2$, although such solubility is low. Therefore, the basicity of the samples decreased in the presence of water during measurement. As a comparison, a well-known solid superbase KNO_3 (20 wt %) modified alumina ($20KNO_3/Al_2O_3$) was employed.[29,30] As demonstrated in Figure 9, the basicity of $20KNO_3/Al_2O_3$ declined rapidly at the beginning of the test and only 38% of the basicity survived after 300 mL·g^{-1} water passed. The good water resistance of CaNS samples results from the low solubility of the basic calcium species in water along with the interaction between the calcium species and the host, which is helpful for expanding the application of solid bases in those processes involving water.

Effect of Guest Species on Mesostructure and Basicity. Apparently, using calcium species as the guest to modify SBA-15 can prepare ordered mesoporous solid superbases in terms of the results mentioned above. However, the

(44) Tanabe, K.; Noyari, R. *Chokyo-san, Chokyo-enki*; Kodansha: Tokyo, 1980, p 114.

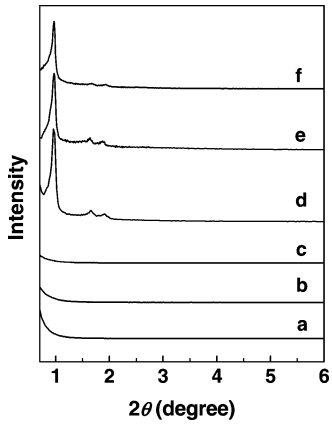

Figure 10. Low-angle XRD patterns of (a) NaNS, (b) KNS, (c) CsNS, (d) MgNS, (e) SrNS, and (f) BaNS. The surface cation density of all the samples is 2.1 cations nm^{-2}; the samples were activated in N_2 at 550 °C before measurement.

modification of SBA-15 with potassium species as the guest only produced composites with weak basicity and a collapsed mesostructure.[31] To explore what causes such great differences between calcium and potassium modified mesoporous silicas in regard to their mesostructure and basicity, a series of metal nitrates from Groups 1 and 2 were employed as guest species to load on mesoporous silica SBA-15. Figure 10 gives the low-angle XRD patterns of these nitrates modified SBA-15, in which quite different patterns were observed. No diffraction peak could be identified from the samples modified by Group 1 metal nitrates, that is, NaNS, KNS, and CsNS, suggesting that the ordered mesostructure of SBA-15 silica was destroyed during activation. However, after being modified by Group 2 metal nitrates, that is, MgNS, SrNS, and BaNS, the samples had three diffraction peaks indexed as (100), (110), and (200) reflections corresponding to *P6mm* hexagonal symmetry, identical to that of SBA-15 and CaNS (Figure 1), which implied the preservation of the ordered mesostructure even if the nitrate was introduced and converted to corresponding basic oxide after activation. Further investigations show that these composites exhibited rather different base strengths. As listed in Table 3, the basic sites formed on Group 1 metal nitrates modified samples possessed low strength, that is, $H_- = 9.3$ for NaNS along with $H_- = 15.0$ for KNS and CsNS. Nevertheless, a high base strength of $H_- = 22.5$ was detected on MgNS, and the superbasicity ($H_- = 27.0$) was generated on CaNS, SrNS, and BaNS composites. Clearly, selecting different guests can promote the formation of strong basic sites on SBA-15 and maintain the original structure of the host, as summarized in Scheme 1.

Discussion

To examine the factors influencing the mesostructure of the composites, the host–guest interaction is first taken into consideration because different guest species may have quite different interaction with the host. In general, the host performs two supporting functions for the guest. It provides a suitable surface to disperse the guest species; also, it should have a considerable interaction with the precursor to form basic sites during activation. The interaction of the host–guest must be moderate because too weak a host–guest interaction may lead to difficulty in both dispersion and decomposition of the base precursor, whereas too strong an interaction causes damage to the host mesostructure. The electronegativity of metal ions (χ_i) in oxide was demonstrated to relate with the interaction between the oxide and the support.[45] Consulting the report of Tanaka and Ozaki,[46] the electronegativity of metal ions in Groups 1 and 2 metal oxides was calculated and listed in Table 3. With the decrease in electronegativity, metal–oxygen contact in the oxide becomes weak, leading to stronger interaction of the oxide with the support.[45] For example, the cation in Cs_2O possesses the lowest electronegativity among the oxides investigated, which results in the strongest interaction of Cs_2O with the silica support. On the contrary, the highest electronegativity of the cation in MgO causes the weakest interaction between guest and host. As is evident in Table 3, the electronegativity of Group 1 metal ions (2.37–2.79) is much lower than that of Group 2 metal ions (4.45–6.55); therefore, the interaction between Group 1 metal oxides and the silica support should be much stronger. Such strong interaction may cause the reaction of basic oxides with the silica support to produce some new compounds similar to silicate during activation. Hence, the mesostructure of the composites modified by Group 1 metal nitrates was unavoidably destroyed. In contrast, the high electronegativity of cations in Group 2 metal oxides is responsible for the good preservation of the mesostructure of the resulting composites.

The mobility of the supported species is considered to be another factor affecting the mesostructure of the composites. If the supported oxide easily diffuses or transfers in the pores of the host at elevated temperature, the potential reaction of these basic oxides with the silica support is accelerated during activation, which is harmful to the preservation of the mesostructure. The Tammann temperature, defined as half the melting point in kelvin, has been proven to be associated with the mobility of the metal ions or atoms in the metal oxide.[47,48] The mobility of the metal ions in the oxide increases rapidly in the vicinity of its Tammann temperature. As listed in Table 3, Group 1 metal oxides possess a much lower Tammann temperature compared to Group 2 metal oxides,[49] suggesting the larger mobility of alkali metal cations in oxides than that of alkaline earth metal cations. In the present study, the activation of the sample is performed at 550 °C to decompose nitrates to corresponding basic oxides. This temperature is higher than the Tammann temperature of Group 1 metal oxides (<430 °C) but lower than that of Group 2 metal oxides (>850 °C), indicating that the cations in Group 1 metal oxides are very "active" during the activation whereas the cations in Group 2 metal

(45) Kumar, M.; Aberuagba, F.; Gupta, J. K.; Rawat, K. S.; Sharma, L. D.; Dhar, G. M. *J. Mol. Catal. A: Chem.* **2004**, *213*, 217.
(46) Tanaka, K. I.; Ozaki, A. *J. Catal.* **1967**, *8*, 1.
(47) Carreon, M. A.; Guliants, V. V. *Eur. J. Inorg. Chem.* **2005**, 27.
(48) Wachs, I. E.; Jehng, J.-M.; Ueda, W. *J. Phys. Chem. B* **2005**, *109*, 2275.
(49) Dean, J. A. *Lange's Handbook of Chemistry*, 15th ed.;Beijing World Publishing Corporation: Beijing, 1999.

Table 3. Physicochemical Properties of Different Nitrates Modified SBA-15 and Corresponding Oxides

	properties of corresponding oxide				
sample[a]	melting point[b] (°C)	Tammann temperature (°C)	metal ionic radius[c] (Å)	electronegativity of metal ion[d] (χ_i)	base strength (H_-)
NaNS	1132	430	0.97	2.79	9.3
KNS	>763	>245	1.33	2.46	15.0
CsNS	490	109	1.67	2.37	15.0
MgNS	2800	1264	0.66	6.55	22.5
CaNS	2900	1314	0.99	5.00	27.0
SrNS	2430	1079	1.12	4.75	27.0
BaNS	1973	850	1.34	4.45	27.0

[a] The surface cation density of all the samples is 2.1 cations nm^{-2}. [b] Data from refs 43 and. 49. [c] Data from ref 50. [d] Calculated according to ref 46.

Scheme 1. Different Structure and Basicity of Mesoporous Silica SBA-15 Modified by Groups 1 and 2 Metal Nitrates

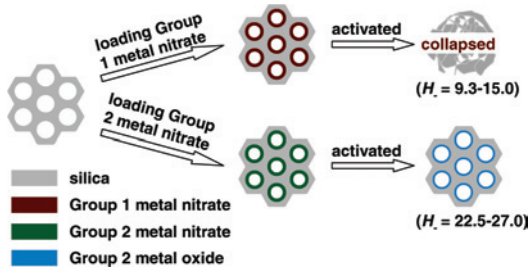

oxides are relatively "stable". Hence, the greater mobility may promote the interaction of Group 1 metal oxides, which are inherently strong basic, with silica support, leading to the damage of the mesostructure of the composites.

Apart from the Tammann temperature of metal oxides, the metal ionic radius is also taken into account to evaluate the impact on the mobility of metal ions and, further, on the mesostructure of the composites. It is generally accepted that the metal ion with the smaller size moves more easily; as a result, the mobility of cations in MgO should be the greatest because of the smallest ionic radius among the cations investigated (Table 3).[50] Accordingly, the ordered mesostructure of MgNS should be easily destroyed in the process of activation. However, the mesostructure of MgNS was well maintained after activation as demonstrated in Figure 10. On the contrary, the mesostructure of CsNS is completely destroyed despite the largest metal ionic radius of Cs_2O. On the basis of these results, it is safe to conclude that the preservation of the mesostructure is related to the interaction between the metal oxide and the silica support along with the mobility of the cations in the metal oxide, which can be characterized by the electronegativity of the metal ions and the Tammann temperature of the metal oxides, respectively; however, no correlation can be proposed between the metal ionic radius of the supported metal oxide and the mesostructure of the composites. These discoveries may be helpful for the selection of guest species to design and synthesize new basic functional materials.

As mentioned above, quite different base strength was measured for the composites loaded with different guests. It is not surprising that low strength (H_- = 9.3–15.0) was detected on Group 1 metal nitrates modified SBA-15 because the reaction of the basic oxides with the silica support resulted in the collapse of the mesostructure and the formation of silicate-like compounds with weak basicity. Although the mesostructure was preserved for all composites by Group 2 metal nitrate modification, strong basicity with strength (H_-) of 22.5 was measured on MgNS whereas superbasicity with strength (H_-) of 27.0 emerged on CaNS, SrNS, and BaNS. Such different basicity originates from the inherent feature of the resulting oxide species because the basicity of an oxide is related to the electron donor property of the oxygen anion.[51] The higher the partial negative charges on the oxygen anions are, the more basic the oxide will be. Hence, the value of the oxygen partial negative charge ($-q_O$), which is estimated from the electronegativity equalization principle,[52] can be taken as a measure of the basicity of an oxide. The $-q_O$ value of MgO (0.50) is obviously lower than that of CaO (0.57), SrO (0.59), and BaO (0.61), [43] which should be responsible for the relatively weaker basicity of MgNS than that of CaNS, SrNS, and BaNS.

Despite great efforts, directly generating the strong basicity on mesoporous silica is still a challenge up to now. Unlike the previous research focusing on the selection of optimal host materials such as alumina or zirconia to disperse potassium species,[29,30] this study reveals the significant effect of the guest and chooses the calcium species as the guest to generate the superbasicity directly on mesoporous silica with good preservation of the ordered mesostructure for the first time. Also, strong basicity can be generated on SBA-15 by using other Group 2 metal nitrates as the guest. Compared with organic base grafting or nitrogen incorporation, alkaline earth metal nitrate modification is a convenient, low-cost, and efficient method to form stronger basicity on mesoporous silica.

Conclusions

(1) A convenient and low-cost method was adopted to directly generate the strong basic sites on mesoporous silica SBA-15 by adjusting the guest species. Strong basicity with strength (H_-) of 22.5 can be formed on magnesium species modified SBA-15, while superbasicity (H_- = 27.0) was generated on the SBA-15 modified with calcium, strontium, and barium species. The ordered mesostructure of these strong bases was maintained well after activation.

(2) The calcium species can be distributed well on the surface of SBA-15. Because of the host–guest interaction,

(50) Lide, D. R. *Handbook of Chemistry and Physics*, 71st ed.; C.R.C. Press: Boca Raton, 1990.

(51) Diez, V. K.; Apesteguia, C. R.; Di Cosimo, J. I. *J. Catal.* **2006**, *240*, 235.

(52) Di Cosimo, J. I.; Diez, V. K.; Apesteguia, C. R. *Appl. Catal., A* **1996**, *137*, 149.

the decomposition of supported calcium nitrate was obviously easier than the bulk one. The CaNS samples possessed good water resistance and high surface areas up to 429 $m^2 \cdot g^{-1}$, which is promising for their potential applications in adsorption and catalysis processes involving water.

(3) Different from the samples of SBA-15 loaded with Group 2 metal nitrates, the composites prepared by Group 1 metal nitrate modification exhibited very weak basicity ($H_- = 9.3–15.0$) and their mesostructure was destroyed completely after activation. Such differences are related to the interaction between the resulting metal oxide and the silica support as well as to the mobility of the cations in the metal oxide, which can be characterized by the electronegativity of the metal ion and the Tammann temperature of the metal oxide, respectively.

Acknowledgment. National Natural Sciences Foundation of China (20673053 and 20773061), Grants 715-04-0120 and 2008AA06Z327 from the 863 Program of the Ministry of Science and Technology of China, National Basic Research Program of China (2007CB613301) and the Analysis Center of Nanjing University financially support this research.

IC702223B